Investigation of the η′N system using the linear sigma model

Sakai, Shuntaro; Jido, Daisuke

PTEP
Prog. Theor. Exp. Phys. **2017**, 013D01 (15 pages)
DOI: 10.1093/ptep/ptw191

Investigation of the $\eta' N$ system using the linear sigma model

Shuntaro Sakai[1,*,†] and Daisuke Jido[2]

[1]*Department of Physics, Kyoto University, Kitashirakawa-Oiwakecho, Kyoto 606-8502, Japan*
[2]*Department of Physics, Tokyo Metropolitan University, Hachioji 192-0397, Japan*
[†]*Present address: Research Center for Nuclear Physics (RCNP), Osaka University, Ibaraki 567-0047, Japan*
[*]E-mail: shsakai@rcnp.osaka-u.ac.jp

Received July 26, 2016; Revised December 3, 2016; Accepted December 16, 2016; Published January 21, 2017

In this paper, we investigate the $\eta' N$ system using the three-flavor linear sigma model including the effect of flavor SU(3) symmetry breaking. The $\eta' N$ bound state is also found in the case including flavor symmetry breaking and coupling with the ηN and πN channels. The $\eta' N$ interaction becomes more attractive with the inclusion of flavor symmetry breaking, which causes mixing between the singlet and octet scalar mesons. The existence of such a bound state would have some impact on the η'–nucleus system, which is of interest from both theoretical and experimental viewpoints.

Subject Index D32

1. Introduction

The properties of the η' meson have attracted continuous attention in hadron physics. Its relatively large mass compared with other low-lying pseudoscalar mesons, such as π or η, is summarized as the $U_A(1)$ problem [1], and many studies [2–5] have been devoted to the role of the $U_A(1)$ anomaly in quantum chromodynamics (QCD) [6–8]. In the three-flavor system, on the other hand, the essential role of chiral symmetry breaking in cooperation with the $U_A(1)$ anomaly for the generation of the η' mass is pointed out in Refs. [9–14].

Partial restoration of chiral symmetry in the nuclear medium attracts our interest; the magnitude of the order parameters of chiral symmetry breaking is expected to be reduced in the nuclear medium [15–17], and its possible effects on hadronic phenomena have been studied intensively (see Ref. [18] for a recent review). In particular, analyses of the pion–nucleus system suggest that such a reduction of the order parameter in the nuclear medium actually occurs with about 30% suppression of the size of the quark condensate at the normal nuclear density [19–22].

Taking account of the partial restoration of chiral symmetry and the strong connection of the η' mass and chiral symmetry breaking, we expect that the mass of the η' meson is reduced in the nuclear medium [14], though the in-medium mass of η' is concerned from the viewpoint of the effective restoration of the $U_A(1)$ symmetry [9,10,23,24]; some model calculations suggest that the η' mass reduces as much as about 100 MeV at the normal nuclear density in association with chiral restoration [25–27]. Then, we expect to find some information on chiral restoration in the nuclear medium through investigation of the η'–nucleus system studied from both theoretical and experimental aspects [28–36].

For the study of the in-medium properties of the η' meson, the interaction between η' and the nucleon N is a basic piece. The $\eta' N$ system is theoretically studied in Refs. [37–40]. Experimentally, analysis of $\pi^- p \to \eta' n$ near the $\eta' n$ threshold suggests the existence of the narrow and shallow $\eta' n$ bound state [41], and a threshold enhancement is seen in the η' photoproduction [42]. On the other hand, recent analysis of the $pp \to pp\eta'$ reaction suggests a small scattering length [43–45].

In our previous study, we investigated the mass of the η' meson in the nuclear medium and the $\eta' N$ two-body interaction in free space using the three-flavor linear sigma model with nucleon [27,46]. Within the leading order of the momentum expansion, we found that the attractive $\eta' N$ interaction is induced by the scalar meson exchange; the $\sigma\eta'\eta'$ coupling is induced by $\mathrm{U}_A(1)$ symmetry breaking, and the transition to the ηN channel is suppressed by the large mass of the octet scalar meson. The $\eta' N$ interaction is strong enough to form the $\eta' N$ bound state. The possible appearance of the bound-state signal in the η' photoproduction process off the deuteron is investigated in Ref. [47].

In this study, we investigate the $\eta' N$ system based on the linear sigma model. Due to the lack of phenomenological information of the $\eta' N$ interaction, we make good use of theoretical considerations and symmetry properties of hadrons. The linear sigma model is one of the well-contained effective models by chiral symmetry and has the mechanism of chiral restoration. In the exploratory stage, it would be interesting to see what comes out from such theoretical analyses. Certainly, once we have experimental information on the $\eta' N$ interaction, we should go to the nonlinear realization of chiral symmetry, in which more phenomenological analyses can be done based on chiral effective theories.

In this paper, we evaluate the $\eta' N$ interaction including the ηN and πN transition at the $\eta' N$ threshold energy, and investigate a possible nucleon resonance dynamically generated from these $\eta' N$, ηN, and πN channels around the $\eta' N$ threshold. A new finding of this study is that transition between the $\eta' N$ and ηN or πN channels are induced by the effect of the $\mathrm{U}(1)_A$ anomaly in addition to the $\eta' N$ elastic channel in this setup. We also take account of the effects of scalar meson mixing caused by the explicit breaking of the flavor SU(3) symmetry, which was not taken into account in the previous work. The mixing induces the octet sigma meson exchange in the $\eta' N$ interaction. We also calculate the mass and width of the possible state of $\eta' N$ by including the scattering channels of ηN and πN.

This paper is constructed as follows: the model used in this calculation is introduced in Sect. 2. The result of the study is given in Sect. 3. Finally, we give a summary and discussion in Sect. 4.

2. Model setup

In this section, we introduce the model used in this study, that is the three-flavor linear sigma model. The Lagrangian is given as follows:

$$\begin{aligned}\mathcal{L} =& \frac{1}{2}\mathrm{tr}(\partial_\mu M \partial^\mu M^\dagger) - \frac{\mu^2}{2}\mathrm{tr}(MM^\dagger) - \frac{\lambda}{4}\mathrm{tr}(MM^\dagger)^2 - \frac{\lambda'}{4}\left[\mathrm{tr}(MM^\dagger)\right]^2 + A\mathrm{tr}(\chi M^\dagger + \chi^\dagger M) \\ &+ \sqrt{3}B(\det M + \det M^\dagger) \\ &+ \bar{N}\left[i\partial\!\!\!/ - m_N - g\left\{\left(\frac{\tilde{\sigma}_0}{\sqrt{3}}\mathbf{1} + \frac{\vec{\sigma}\cdot\vec{\tau}}{\sqrt{2}} + \frac{\tilde{\sigma}_8}{\sqrt{6}}\mathbf{1}\right) + i\gamma_5\left(\frac{\eta_0}{\sqrt{3}}\mathbf{1} + \frac{\vec{\pi}\cdot\vec{\tau}}{\sqrt{2}} + \frac{\eta_8}{\sqrt{6}}\mathbf{1}\right)\right\}\right]N, \quad (1)\end{aligned}$$

where

$$M = M_s + M_{ps}, \quad (2)$$

$$M_s = \begin{pmatrix} \frac{\sigma_0}{\sqrt{3}} + \frac{\sigma_3}{\sqrt{2}} + \frac{\sigma_8}{\sqrt{6}} & a^+ & \kappa^+ \\ a^- & \frac{\sigma_0}{\sqrt{3}} - \frac{\sigma_3}{\sqrt{2}} + \frac{\sigma_8}{\sqrt{6}} & \kappa^0 \\ \kappa^- & \bar{\kappa}^0 & \frac{\sigma_0}{\sqrt{3}} - \sqrt{\frac{2}{3}}\sigma_8 \end{pmatrix}, \tag{3}$$

$$M_{ps} = \begin{pmatrix} \frac{\eta_0}{\sqrt{3}} + \frac{\pi_3}{\sqrt{2}} + \frac{\eta_8}{\sqrt{6}} & \pi^+ & K^+ \\ \pi^- & \frac{\eta_0}{\sqrt{3}} - \frac{\pi_3}{\sqrt{2}} + \frac{\eta_8}{\sqrt{6}} & K^0 \\ K^- & \bar{K}^0 & \frac{\eta_0}{\sqrt{3}} - \sqrt{\frac{2}{3}}\eta_8 \end{pmatrix}, \tag{4}$$

$$N = {}^t(p, n), \tag{5}$$

$$\chi = \sqrt{3}\mathrm{diag}(m_u, m_d, m_s) = \sqrt{3}\mathrm{diag}(m_q, m_q, m_s). \tag{6}$$

The Gell-Mann matrix λ_a and Pauli matrix τ_a satisfy the normalization $\mathrm{tr}(\lambda_a\lambda_b) = 2\delta_{ab}$ and $\mathrm{tr}(\tau_a\tau_b) = 2\delta_{ab}$, respectively. $\tilde{\sigma}_i$ $(i = 0, 8)$ means the fluctuation from its mean field, which will be explained later. The meson and baryon fields belong to the $(\mathbf{3}, \bar{\mathbf{3}}) \oplus (\bar{\mathbf{3}}, \mathbf{3})$ representation of $\mathrm{SU}(3)_L \times \mathrm{SU}(3)_R$ and the Lagrangian is constructed to be invariant under the chiral transformation. The isospin symmetry is implemented by the degenerate u and d quark masses $m_q = m_u = m_d$, and the flavor symmetry breaking appears from the non-degenerate strange quark mass, $m_s \neq m_q$. For the baryonic part of the Lagrangian, the irrelevant hyperons in this study are omitted.

The vacuum is determined so as to minimize the effective potential obtained with the tree-level approximation in this study. The effective potential $V_\sigma(\sigma_0, \sigma_8)$ is given as

$$\begin{aligned} V_\sigma(\sigma_0, \sigma_8) = {} & \frac{\mu^2}{2}(\sigma_0^2 + \sigma_8^2) + \frac{\lambda}{12}(\sigma_0^4 + 6\sigma_0^2\sigma_8^2 - 2\sqrt{2}\sigma_0\sigma_8^3 + \frac{3}{2}\sigma_8^4) + \frac{\lambda'}{4}(\sigma_0^2 + \sigma_8^2)^2 \\ & - \frac{2}{3}B(\sigma_0 + \frac{\sigma_8}{\sqrt{2}})^2(\sigma_0 - \sqrt{2}\sigma_8) - 2A(2m_q(\sigma_0 + \frac{\sigma_8}{\sqrt{2}}) + m_s(\sigma_0 - \sqrt{2}\sigma_8)). \end{aligned} \tag{7}$$

The order parameter of the chiral symmetry breaking is the expectation value of the neutral scalar meson fields σ_i $(i = 0, 8)$. The expectation value of σ_3 vanishes due to the isospin symmetry. Here, we decompose them into the mean field value $\langle\sigma_i\rangle$ and fluctuation $\tilde{\sigma}_i$; $\sigma_i = \langle\sigma_i\rangle + \tilde{\sigma}_i$. The minimum conditions of the effective potential $\partial V_\sigma/\partial\sigma_{0,8} = 0$ are satisfied for the expectation values of $\sigma_{0,8}$. The expectation values are related to the meson decay constants; at the tree level they are given as $f_\pi = \sqrt{2/3}\langle\sigma_0\rangle + \langle\sigma_8\rangle/\sqrt{3}$ and $f_K = \sqrt{2/3}\langle\sigma_0\rangle - \langle\sigma_8\rangle/2\sqrt{3}$. The non-zero vacuum expectation value $\langle\sigma_0\rangle$ is responsible for the spontaneous breaking of chiral symmetry in the linear sigma model, while the finite vacuum expectation value $\langle\sigma_8\rangle$ is caused by the explicit flavor symmetry breaking due to the non-degenerate strange quark mass.

The parameters contained in the meson part and $\langle\sigma_0\rangle$ and $\langle\sigma_8\rangle$ are determined to reproduce the observed masses and decay constants of mesons. The parameter in the nucleon part g is fixed in order for the magnitude of the quark condensate to reduce by 35% at the normal nuclear density, which is suggested from analysis of the deeply bound state of the pionic atom [19]. Details of the determination of the parameters are given in Ref. [27]. The input and determined parameters are given in Tables 1 and 2, respectively. The masses of the mesons used as input parameters come from the values in Ref. [48]. The masses of the π and K mesons are obtained with the isospin average.

Here, we treat the mass of the σ meson m_σ as an input parameter. The dependence on m_σ of our result will be discussed later.

The mass eigenstates of the neutral mesons are different from the eigenstates of the flavor appearing in the Lagrangian (1) due to the flavor symmetry breaking from the difference between m_q and m_s in

Table 1. The input parameters for the determination of the parameters in the Lagrangian. These values are taken from Ref. [48]. The masses of π and K are isospin-averaged values.

f_π [MeV]	f_K [MeV]	m_π [MeV]	m_K [MeV]
92.2	110.4	138.04	495.64
	$m_\eta^2 + m_{\eta'}^2$ [MeV^2]	m_σ [MeV]	
	$547.85^2 + 957.78^2$	700	

Table 2. The determined parameters in the Lagrangian.

$\langle\sigma_0\rangle$ [MeV]	$\langle\sigma_8\rangle$ [MeV]	μ^2 [MeV^2]	λ [–]
127.78	-21.02	4.21×10^4	58.80
λ' [-]	A [MeV^2]	B [MeV]	g [–]
2.46	7.17×10^4	997.95	9.84

the Lagrangian. The mass eigenstates of the isospin singlet scalar (pseudoscalar) mesons are denoted by σ and f_0 (η' and η). They are related by

$$\begin{pmatrix} \sigma \\ f_0 \end{pmatrix} = \begin{pmatrix} \cos\theta_s & \sin\theta_s \\ -\sin\theta_s & \cos\theta_s \end{pmatrix} \begin{pmatrix} \sigma_0 \\ \sigma_8 \end{pmatrix}, \tag{8}$$

$$\begin{pmatrix} \eta' \\ \eta \end{pmatrix} = \begin{pmatrix} \cos\theta_{ps} & \sin\theta_{ps} \\ -\sin\theta_{ps} & \cos\theta_{ps} \end{pmatrix} \begin{pmatrix} \eta_0 \\ \eta_8 \end{pmatrix}, \tag{9}$$

where θ_s and θ_{ps} are the mixing angles in the scalar and pseudoscalar sectors, respectively. The matrices (8) and (9) diagonalize the mass matrices written in the bases of $\sigma_{0,8}$ and $\eta_{0,8}$, respectively. The mass matrices are related by

$$(\sigma, f_0) \begin{pmatrix} m_\sigma^2 & 0 \\ 0 & m_{f_0}^2 \end{pmatrix} \begin{pmatrix} \sigma \\ f_0 \end{pmatrix} = (\sigma_0, \sigma_8) \begin{pmatrix} m_{\sigma_0}^2 & m_{\sigma_0\sigma_8}^2 \\ m_{\sigma_0\sigma_8}^2 & m_{\sigma_8}^2 \end{pmatrix} \begin{pmatrix} \sigma_0 \\ \sigma_8 \end{pmatrix}, \tag{10}$$

$$(\eta', \eta) \begin{pmatrix} m_{\eta'}^2 & 0 \\ 0 & m_\eta^2 \end{pmatrix} \begin{pmatrix} \eta' \\ \eta \end{pmatrix} = (\eta_0, \eta_8) \begin{pmatrix} m_{\eta_0}^2 & m_{\eta_0\eta_8}^2 \\ m_{\eta_0\eta_8}^2 & m_{\eta_8}^2 \end{pmatrix} \begin{pmatrix} \eta_0 \\ \eta_8 \end{pmatrix}. \tag{11}$$

The explicit form of the meson mass is given in Appendix A. The off-diagonal part of the matrices, which causes the transition between the singlet and octet mesons, appears from the explicit flavor symmetry breaking. The mixing angles are found as $\theta_s = 21.0^\circ$ and $\theta_{ps} = -6.2^\circ$ in the case of $m_\sigma = 700$ MeV. The masses of the scalar mesons, σ, f_0, and a_0 are obtained as 700, 1286, and 1071 MeV, respectively.

3. Results

In this section, we show the results of this study. We first show the $\eta' N$ interaction and then the T matrix of $\eta' N$ with the coupling to the ηN and πN channels including the effect of the flavor SU(3) symmetry breaking. The effect of the flavor symmetry breaking appears from the nonzero value of $\langle\sigma_8\rangle$. This leads to the modification of the meson coupling and the mixing property of mesons. While the $\pi\pi N$ can give significant effects in general, we omit it following the discussion given in Ref. [40]; the calculation in Ref. [49] suggests the minor correction for the $I = 1/2$ channel amplitude due to the $\pi\pi N$ channel, while the $\eta' N$ channel is not included in the study.

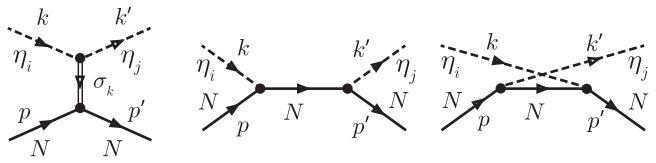

Fig. 1. Diagrams taken into account in this study. The solid, double solid, and dashed lines mean the nucleon, scalar meson, and pseudoscalar meson. $\eta_{i,j} = \pi, \eta, \eta'$ and $\sigma_k = \sigma, f_0, a_0$.

3.1. $\eta' N$ interaction

First, we evaluate the $\eta' N$, ηN, and πN interactions. Here, the matrix element of the interaction is evaluated within the tree-level approximation. The diagrams included for the evaluation of the $\eta' N$ interaction are shown in Fig. 1. Here, η_i and η_j are the mesons in the initial and final states ($\eta_{i,j} = \pi, \eta, \eta'$). The matrix elements are calculated as follows:

$$\mathcal{M}_{\eta_i N \to \eta_j N} = \bar{u}(p', s') \left[\frac{g_{\sigma_k \eta_i \eta_j} g_{\sigma_k N}}{q^2 - m_{\sigma_k}^2 + i\epsilon} + \frac{g_{\eta_i N} g_{\eta_j N} \not{k}}{(p+k)^2 - m_N^2 + i\epsilon} - \frac{g_{\eta_i N} g_{\eta_j N} \not{k}'}{(p-k')^2 - m_N^2 + i\epsilon} \right] u(p, s), \tag{12}$$

where p (p'), and k (k') are the momenta of the incoming (outgoing) nucleon and meson in the center-of-mass frame, respectively, which are explicitly written as

$$p^\mu = (E_N = \sqrt{p_{cm}^2 + m_N^2}, 0, 0, p_{cm}), \tag{13}$$

$$k^\mu = (E_i = \sqrt{p_{cm} + m_i^2}, 0, 0, -p_{cm}), \tag{14}$$

$$p'^\mu = (E'_N = \sqrt{p'^2_{cm} + m_N^2}, p'_{cm} \sin\theta, 0, p'_{cm} \cos\theta), \tag{15}$$

$$k'^\mu = (E_j = \sqrt{p'^2_{cm} + m_j^2}, -p'_{cm} \sin\theta, 0, -p'_{cm} \cos\theta), \tag{16}$$

where m_i and m_j are the masses of the pseudoscalar mesons η_i and η_j, respectively, and p_{cm} and p'_{cm} are the momenta of hadrons in the initial and final states in the center-of-mass frame. They are given by $p_{cm} = \frac{1}{2W}\sqrt{\lambda(W^2, m_N^2, m_i^2)}$ and $p'_{cm} = \frac{1}{2W}\sqrt{\lambda(W^2, m_N^2, m_j^2)}$, with $\lambda(x, y, z) = x^2 + y^2 + z^2 - 2xy - 2yz - 2zx$ and the center-of-mass energy $W = E_N + E_i$. Here, we assume that the initial particles come along with the z-axis. In Eq. (12), q denotes the momentum transfer defined as $q = p' - p$. Here, we write the total momentum of the system as $P^\mu = p^\mu + k^\mu = (W, 0, 0, 0)$. The coupling strengths of the hadrons, $\eta_i(\sigma_i)\bar{N}N$ and $\sigma_k \eta_i \eta_j$, are denoted as $g_{\eta_i(\sigma_i)N}$ and $g_{\sigma_k \eta_i \eta_j}$. Their explicit expressions are given in Appendix C.

We solve the scattering equation with the s-wave interaction deduced from the matrix element Eq. (12). For this purpose, we introduce the s-wave interaction vertex $V_{\eta_i N \to \eta_j N}$ defined by

$$V_{\eta_i N \to \eta_j N} = \frac{1}{2} \sum_{\text{spin}} \frac{1}{2} \int_{-1}^{1} d(\cos\theta) \mathcal{M}_{\eta_i N \to \eta_j N}. \tag{17}$$

Here, we have performed s-wave projection and taken spin average for the initial nucleon and spin sum over the final nucleon. The s-wave component would be dominant near the $\eta' N$ threshold that we are focusing on. Moreover, we take the $I = 1/2$ component of the πN channel, which can couple to the $\eta' N$ channel. The explicit form of $V_{\eta_i N \to \eta_j N}$ is given in Appendix B, and the value at the $\eta' N$

Table 3. Values of $V_{i\to j}$ at the $\eta' N$ threshold. For the πN channel, the projection into $I = 1/2$ is done.

$V_{\eta' N\to\eta' N}$ [MeV^{-1}]	$V_{\eta N\to\eta N}$ [MeV^{-1}]	$V_{\pi N\to\pi N}$ [MeV^{-1}]
-7.14×10^{-2}	2.02×10^{-2}	-8.54×10^{-3}
$V_{\eta' N\to\eta N}$ [MeV^{-1}]	$V_{\eta' N\to\pi N}$ [MeV^{-1}]	$V_{\eta N\to\pi N}$ [MeV]$^{-1}$
9.92×10^{-3}	5.67×10^{-2}	1.74×10^{-2}

threshold is presented in Table 3. $V_{\eta_i N\to\eta_j N}$ is evaluated using the physical value of the nucleon and pseudoscalar mesons.

Comparing the value of the s-wave $\eta' N$ interaction obtained in this calculation with that obtained in Refs. [27,46], where the flavor symmetry breaking is not incorporated in the calculation of the $\eta' N$ interaction, we find that the present value of $V_{\eta' N\to\eta' N}$ is larger than the previous calculation, in which we have obtained $V_{\eta' N\to\eta' N} = -0.054$ and $V_{\eta' N\to\eta N} = 0.012\,\text{MeV}^{-1}$, which are evaluated also without the meson mixing and under the momentum expansion. As demonstrated in Refs. [27,46], the scalar meson exchange has the leading contribution in the momentum expansion in these channels. This result implies that the SU(3) flavor symmetry breaking and the resultant scalar meson mixing give substantial effects on the $\eta' N$ interaction. In particular, the parameter g which characterizes the coupling of the σ meson and nucleon is larger when we take account of the mixing effect.

Next, we comment on the effect of the η–η' mixing. As we mentioned in the previous section, the mixing angle between η' and η is as small as $-6.2°$. If we omit the mixing between the η and η' mesons, $V_{\eta' N\to\eta' N}$, $V_{\eta' N\to\eta N}$, $V_{\eta' N\to\pi N}$, $V_{\eta N\to\eta N}$, and $V_{\eta N\to\pi N}$ are given as -0.068, 0.020, 0.058, 0.017, and $0.011\,\text{MeV}^{-1}$, respectively, where the mixing effect does not affect $V_{\pi N\to\pi N}$. With the omission of the pseudoscalar mixing, the η' and η correspond to the flavor eigenstates η_0 and η_8, respectively. The modification by the η–η' mixing appears to be small compared with the values in Table 3.

3.2. $\eta' N$ system

We evaluate the T matrix of the $\eta' N$ system by solving the scattering equation,

$$T_{i\to j} = V_{i\to j} + V_{i\to k} G_k T_{k\to j}, \tag{18}$$

where i, j, and k mean πN, ηN, or $\eta' N$, and the s-wave projection and the spin average is used to obtain the interaction kernel of the scattering equation $V_{i\to j}$. Here, we use the value of $V_{i\to j}$ evaluated at the $\eta' N$ threshold to evaluate $T_{i\to j}$. The scattering equation can be solved in an algebraic way: $T_{i\to j} = [(1 - VG)^{-1} V]_{ij}$. The loop function G_i in the equation which has an ultraviolet divergence is regularized by the use of the dimensional regularization. Then, G_i is written as follows:

$$\begin{aligned} G_i(W) =& i\int \frac{d^4q}{(2\pi)^4} \frac{2m_N}{(P-q)^2 - m_N^2 + i\epsilon} \frac{1}{q^2 - m_P^2 + i\epsilon} \\ =& \frac{2m_N}{(4\pi)^2}\left[a_i(\mu) + \ln\left(\frac{m_N^2}{\mu^2}\right) + \frac{W^2 - m_N^2 + m_P^2}{2W^2}\ln\left(\frac{m_P^2}{m_N^2}\right) \right. \\ &+ \frac{p_{cm}}{W}\left\{ \ln(W^2 - m_N^2 + m_P^2 + 2p_{cm}W) + \ln(W^2 + m_N^2 - m_P^2 + 2p_{cm}W) \right. \\ &\left.\left. - \ln(-W^2 - m_N^2 + m_P^2 + 2p_{cm}W) - \ln(-W^2 + m_N^2 - m_P^2 + 2p_{cm}W) \right\} \right], \end{aligned} \tag{19}$$

Table 4. The values of the pole position, scattering length, and couplings of the bound state with the channel i, g_{iN^*}, with $m_\sigma = 700$ MeV.

Pole position [MeV]	Binding energy [MeV]
$1839.7 - 7.2i$	$57.0 - 7.2i$
Scattering length [fm]	Effective range [fm]
$-0.98 + 5.7 \times 10^{-2} i$	$0.22 - 6.8 \times 10^{-3} i$

$g_{\eta' NN^*}$ [–]	$g_{\eta NN^*}$ [–]	$g_{\pi NN^*}$ [–]
$4.1 + 0.15i$	$-0.38 + 0.25i$	$-0.32 + 1.7 \times 10^{-2} i$

where m_N and m_P are the masses of the nucleon and the pseudoscalar meson, and μ is a renormalization point which is fixed as $\mu = m_N$ in this calculation. The subtraction constant $a_i(\mu)$ is determined with the natural renormalization scheme [50]; this implies that the contribution from other degrees of freedom than those contained in this model is excluded. The values of the subtraction constants are $a_{\eta' N}(m_N) = -1.838$, $a_{\eta N}(m_N) = -1.239$, and $a_{\pi N}(m_N) = -0.398$.

It is known that the linear sigma model is even less suitable for the πN system with energies far from the πN threshold. The present model may not control the πN system well. Actually, evaluating the cross section of $\pi^+ n \to \eta' p$ using the T matrix obtained in this model, we find that the model substantially overestimates the transition cross section reported in Ref. [51]; the cross section is evaluated as about 1.3 mb, which is about ten times larger than the value in Ref. [51]. To control the transition strength to the πN channel, we scale down the vertex $V_{\pi N \to \eta' N}$ so as to reproduce the experimental data, $\sigma_{\pi^+ n \to \eta' p} = 0.1$ mb at $W = 2$ GeV. This can be achieved by multiplying a factor $x_{13} = 0.153$ to the vertex $V_{\pi N \to \eta' N}$ for $m_\sigma = 700$ MeV.

To obtain the mass and width of the $\eta' N$ bound (or resonance) state, we perform analytic continuation of the obtained T matrix to the complex energy plane and find a pole of the T matrix. From the pole residue, we can obtain the coupling of the hadrons in the channel i and the bound state g_{iN^*}. Near the pole of $T_{i \to j}$, we can write $T_{i \to j}$ as

$$T_{i \to j} = \frac{g_{iN^*} g_{jN^*}}{W - m_R} + (\text{regular part at } W = m_R), \tag{20}$$

where the complex value m_R denotes the pole position of the T matrix.

The binding energy, scattering length of $\eta' N$, and the coupling of the bound state with the channel i, g_{iN^*}, with $m_\sigma = 700$ MeV are given in Table 4. The definitions of the scattering length a and effective range r_e are the same as those in Ref. [52]:

$$a = -\frac{m_N}{4\pi W} T(W)\Big|_{W = m_N + m_P}, \tag{21}$$

$$r_e = \frac{d^2}{dk^2} \left(-\frac{m_N}{4\pi W} T(W) \right)^{-1} \Bigg|_{W = m_N + m_P}, \tag{22}$$

where the momentum of a meson in the center-of-mass frame k and the center-of-mass energy W are related by $k = \frac{1}{2W} \sqrt{[W^2 - (m_N + m_P)^2][W^2 - (m_N - m_P)^2]}$. m_N and m_P are the masses of the nucleon and pseudoscalar meson, respectively. A plot of the absolute value, real part, and imaginary part of the T matrix in the $\eta' N$ elastic channel $T_{\eta' N \to \eta' N}$ is shown in Fig. 2. One can see a clear peak in the $\eta' N$ bound state in $\left| T_{\eta' N \to \eta' N} \right|$.

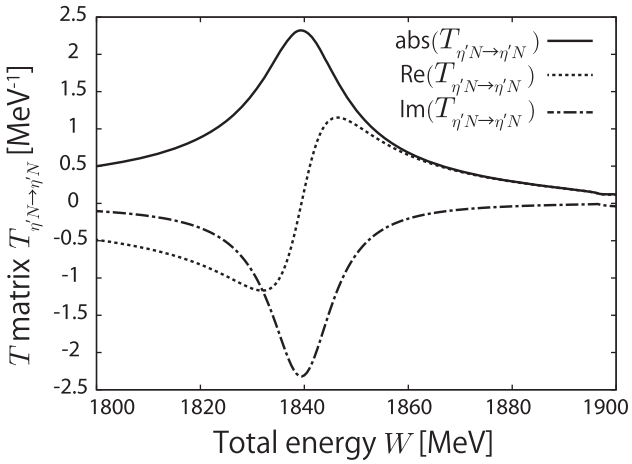

Fig. 2. Plot of the absolute value, real part, and imaginary part of the T matrix in the $\eta' N$ channel with $m_\sigma = 700$ MeV. The solid, dashed, and dash-dotted lines stand for the absolute value, real part, and imaginary part of the T matrix $T_{\eta'N\to\eta'N}$, respectively.

Table 5. The pole position of the $\eta' N$ bound state varying the mass of the scalar meson m_σ.

m_σ [MeV]	pole position [MeV]	binding energy [MeV]	x_{13} [–]
610	$1822.1 - 3.6i$	$74.6 - 3.6i$	0.21
656	$1830.8 - 4.5i$	$65.9 - 4.5i$	0.165
700	$1839.7 - 7.2i$	$57.0 - 7.2i$	0.153
743	$1848.0 - 10.6i$	$48.7 - 10.6i$	0.15

In this model we can treat the mass of the σ meson as an input parameter, as mentioned in Sect. 2. In the chiral effective theory in the nonlinear realization, the sigma meson mass should be irrelevant for low-energy dynamics. Varying the mass of the sigma meson m_σ, we can find a pole of the $\eta' N$ bound state. The pole position and the scale factor x_{13} for the fit of $\sigma_{\pi^+ n\to\eta' p}$ with the change of the σ mass are given in Table 5. The binding energy of the $\eta' N$ system is slightly sensitive to the sigma meson mass, and is roughly varied from 75 to 45 MeV, and the imaginary part of the pole position from -4 to -10 MeV with the change of m_σ from 600 to 750 MeV.

4. Summary and discussion

In this paper, we investigate the $\eta' N$ system using the three-flavor linear sigma model. The $\eta' N$ interaction is evaluated using the tree-level amplitude from the linear σ model including the effect of the flavor symmetry breaking. The effect of the πN channel is phenomenologically taken into account to reproduce the experimental data given in Ref. [51]. We also find an $\eta' N$ bound state if the flavor symmetry breaking is taken into account; the attractive interaction of $\eta' N$ becomes stronger because the coupling of the sigma meson and nucleon becomes stronger with the inclusion of the mixing effect. The parameter g which controls the strength of the coupling between the sigma meson and nucleon is larger than that without the mixing effect. In this study, the effect of the transition to the ηN and πN channel does not seem to be so large because the imaginary part of the pole is relatively small compared with its real part. The attractive $\eta' N$ interaction and the possible bound state appearing from the sigma exchange contribution in association with the $U_A(1)$ anomaly would be suggestive for future theoretical and experimental studies about the properties of the η'

meson. In such studies, a phenomenological approach based on nonlinear sigma models respecting the experimental data with the inclusion of the πN and ηN channels should be followed.

As we have commented in the text, the exchanges of the scalar mesons cause the transitions of the $\eta' N$ into the other channels. There may be room for consideration of the inclusion of the $K\Lambda$ and $K\Sigma$ channels; the transitions into these channels can appear from the exchange of the strange scalar meson, e.g., the κ meson in this model. Then, the investigation of the possible effect from these channels remains as a future task while we have concentrated on the non-strange hadrons in this study.

The existence of such a bound state would have some impact on the spectrum of the η'-nucleus system studied in Refs. [26,28–31]; the existence of the bound state generally gives the energy dependence to the η'–optical potential in the nuclear medium. Then, the expected spectrum of the η'–nucleus system studied in Refs. [26,28–31] would be modified if one takes account of the possible $\eta' N$ bound state.

Acknowledgements

S. S. was a JSPS fellow and appreciates the support of JSPS Grant-in-Aid No. 25-1879. The work of D. J. was partly supported by Grant-in-Aid for Scientific Research from JSPS 25400254.

Appendix A. Meson mass

The explicit form of the meson mass is given in this appendix. The mass of the scalar and pseudoscalar mesons in the basis of the Gell-Mann matrix are summarized in Table A.1. Here, we parameterize the squared meson mass m^2 as

$$m^2 = c_\mu \mu^2 + c_\lambda \lambda + c_{\lambda'} \lambda' + c_B B, \tag{A1}$$

and the coefficients c_μ, c_λ, $c_{\lambda'}$, and c_B for each meson are presented in the table. The transitions between the isovector and isoscalar mesons, σ_3 and $\sigma_{0,8}$ or π_3 and $\eta_{0,8}$, are suppressed by the isospin symmetry. The masses of the neutral mesons σ, f_0 and η, η' are obtained as the eigenvalues of the mass matrices defined in Eqs. (8) and (9). They are given as $m^2_{\sigma/f_0} = \frac{1}{2}(m^2_{\sigma_0} + m^2_{\sigma_8} \mp \sqrt{(m^2_{\sigma_0} - m^2_{\sigma_8})^2 + 4(m^2_{\sigma_0\sigma_8})^2})$ and $m^2_{\eta'/\eta} = \frac{1}{2}(m^2_{\eta_0} + m^2_{\eta_8} \pm \sqrt{(m^2_{\eta_0} - m^2_{\eta_8})^2 + 4(m^2_{\eta_0\eta_8})^2})$. Using the meson masses, the mixing angles of the scalar and pseudoscalar sectors, θ_s and θ_{ps}, are given by $\tan 2\theta_s = 2m^2_{\sigma_0\sigma_8}/(m^2_{\sigma_0} - m^2_{\sigma_8})$ and $\tan 2\theta_{ps} = 2m^2_{\eta_0\eta_8}/(m^2_{\eta_0} - m^2_{\eta_8})$.

Table A.1. Table of the meson mass. The squared mass of the meson m^2 is parameterized as $m^2 = c_\mu \mu^2 + c_\lambda \lambda + c_{\lambda'} \lambda' + c_B B$.

meson	c_μ	c_λ	$c_{\lambda'}$	c_B
$m^2_{\sigma_0}$	1	$\langle\sigma_0\rangle^2 + \langle\sigma_8\rangle^2$	$3\langle\sigma_0\rangle^2 + \langle\sigma_8\rangle^2$	$-4\langle\sigma_0\rangle$
$m^2_{\sigma_3}$	1	$(\langle\sigma_0\rangle + \frac{\langle\sigma_8\rangle}{\sqrt{2}})^2$	$\langle\sigma_0\rangle^2 + \langle\sigma_8\rangle^2$	$2(\langle\sigma_0\rangle - \sqrt{2}\langle\sigma_8\rangle)$
$m^2_{\sigma_8}$	1	$\langle\sigma_0\rangle^2 - \sqrt{2}\langle\sigma_0\rangle\langle\sigma_8\rangle + \frac{3}{2}\langle\sigma_8\rangle^2$	$\langle\sigma_0\rangle^2 + 3\langle\sigma_8\rangle^2$	$2(\langle\sigma_0\rangle + \sqrt{2}\langle\sigma_8\rangle)$
$m^2_{\sigma_0\sigma_8}$	0	$\frac{1}{2}\langle\sigma_8\rangle(4\langle\sigma_0\rangle - \sqrt{2}\langle\sigma_8\rangle)$	$2\langle\sigma_0\rangle\langle\sigma_8\rangle$	$2\langle\sigma_8\rangle$
$m^2_{\eta_0}$	1	$\frac{1}{3}(\langle\sigma_0\rangle^2 + \langle\sigma_8\rangle^2)$	$\langle\sigma_0\rangle^2 + \langle\sigma_8\rangle^2$	$4\langle\sigma_0\rangle$
$m^2_{\pi_3}$	1	$\frac{1}{3}(\langle\sigma_0\rangle^2 + \sqrt{2}\langle\sigma_0\rangle\langle\sigma_8\rangle + \frac{\langle\sigma_8\rangle^2}{2})$	$\langle\sigma_0\rangle^2 + \langle\sigma_8\rangle^2$	$-2(\langle\sigma_0\rangle - \sqrt{2}\langle\sigma_8\rangle)$
$m^2_{\eta_8}$	1	$\frac{1}{3}(\langle\sigma_0\rangle^2 - \sqrt{2}\langle\sigma_0\rangle\langle\sigma_8\rangle + \frac{3}{2}\langle\sigma_8\rangle^2)$	$\langle\sigma_0\rangle^2 + \langle\sigma_8\rangle^2$	$-2(\langle\sigma_0\rangle + \sqrt{2}\langle\sigma_8\rangle)$
$m^2_{\eta_0\eta_8}$	0	$\frac{2}{3}\langle\sigma_8\rangle(\langle\sigma_0\rangle - \frac{\langle\sigma_8\rangle}{2\sqrt{2}})$	0	$-2\langle\sigma_8\rangle$

Appendix B. Form of $V_{i\to j}$

In this appendix, we present the explicit form of the interaction kernel of the scattering equation. As given in Eq. (17), we apply the s-wave projection and the average of the initial state nucleon. The couplings $g_{\sigma_i N}$, $g_{\eta_i N}$, and $g_{\sigma_i\eta_j\eta_k}$ ($\eta_i = \pi_3, \eta_0, \eta_8$ and $\sigma_i = \sigma_0, \sigma_3, \sigma_8$) appearing in the following equations are given in Appendix C.

Here, p, k, p', and k' are the four momenta of the initial-state nucleon, the initial-state meson, the final-state nucleon, and the final-state meson in the center-of-mass frame which are given in Eqs. (13)–(16). The matrix element of $\eta_i N \to \eta_j N$ in the tree level is written as follows:

$$\mathcal{M}_{\eta_i N\to\eta_j N} = \bar{u}(p',s')\left[\frac{g_{\sigma_k\eta_i\eta_j}g_{\sigma_k N}}{q^2 - m_{\sigma_k}^2 + i\epsilon} + \frac{g_{\eta_i N}g_{\eta_j N}\not{k}}{(p+k)^2 - m_N^2 + i\epsilon} - \frac{g_{iN}g_{jN}\not{k}'}{(p-k')^2 - m_N^2 + i\epsilon}\right]u(p,s). \tag{B1}$$

First, $\frac{1}{2}\sum_{s,s'}\bar{u}(p',s')\not{k}u(p,s)$ is written as

$$\frac{1}{2}\sum_{s,s'}\bar{u}(p',s')\not{k}u(p,s) = \frac{\sqrt{(E_N+m_N)(E'_N+m_N)}}{2m_N} \cdot\left[E_i + \frac{p_{cm}^2}{E_N+m_N} + (E_i+E_N+m_N)\frac{p_{cm}p'_{cm}\cos\theta}{(E_N+m_N)(E'_N+m_N)}\right], \tag{B2}$$

where the Dirac spinor $u(p,s)$ is normalized as $\bar{u}(p,s')u(p,s) = \delta_{ss'}$ and χ_s is the Pauli spinor normalized as $\chi^\dagger_{s'}\chi_s = \delta_{ss'}$. In the same way, $\frac{1}{2}\sum_{s,s'}\bar{u}(p',s')\not{k}'u(p,s)$ is written as

$$\frac{1}{2}\sum_{s,s'}\bar{u}(p',s')\not{k}'u(p,s) = \frac{\sqrt{(E_N+m_N)(E'_N+m_N)}}{2m_N} \cdot\left[E_j + \frac{p_{cm}'^2}{E'_N+m_N} + (E_j+E'_N+m_N)\frac{p_{cm}p'_{cm}\cos\theta}{(E_N+m_N)(E'_N+m_N)}\right]. \tag{B3}$$

Moreover, $\frac{1}{2}\sum_{s,s'}\bar{u}(p,s')u(p,s)$ is written as

$$\frac{1}{2}\sum_{s,s'}\bar{u}(p',s')u(p,s) = \frac{\sqrt{(E_N+m_N)(E'_N+m_N)}}{2m_N}\left(1 - \frac{p_{cm}p'_{cm}\cos\theta}{(E_N+m_N)(E'_N+m_N)}\right). \tag{B4}$$

Substituting the explicit form of p, k, p', and k' in Eqs. (13)–(16), the matrix element is written as

$$\begin{aligned}\frac{1}{2}\sum_{s,s'}\mathcal{M}_{\eta_i N\to\eta_j N} = \frac{\sqrt{(E_N+m_N)(E'_N+m_N)}}{2m_N}\Bigg[&\sum_{\sigma_k}\frac{g_{\sigma_k N}g_{\sigma_k\eta_i\eta_j}}{2p_{cm}p'_{cm}\cos\theta - m_{\sigma_k}^2 + 2m_N^2 - 2E_N E'_N} \\ &+ \frac{g_{\eta_i N}g_{\tau_j N}}{W^2 - m_N^2 + i\epsilon}\left(E_i + \frac{p_{cm}^2}{E_N+m_N} + (E_i+E_N+m_N)\frac{p_{cm}p'_{cm}\cos\theta}{(E_N+m_N)(E'_N+m_N)}\right) \\ &+ \frac{g_{\eta_i N}g_{\eta_j N}}{2(E_N E_j + p_{cm}p'_{cm}\cos\theta) - m_j^2}\Bigg(E_j + \frac{p_{cm}'^2}{E'_N+m_N} \\ &+ (E_j+E'_N+m_N)\frac{p_{cm}p'_{cm}\cos\theta}{(E_N+m_N)(E'_N+m_N)}\Bigg)\Bigg].\end{aligned} \tag{B5}$$

With the s-wave projection $\frac{1}{2}\int_{-1}^{1} d\cos\theta$, the matrix element is written as

$$\frac{1}{2}\int_{-1}^{1} d(\cos\theta)\frac{1}{2}\sum_{s,s'}\mathcal{M}_{\eta_i N\to\eta_j N} = \frac{\sqrt{(E_N+m_N)(E'_N+m_N)}}{2m_N}\left[\sum_{\sigma_k}\left\{-\frac{1}{2(E'_N+m_N)(E_N+m_N)}\right.\right.$$
$$+\frac{1}{4p_{cm}p'_{cm}}\left(1-\frac{m^2_{\sigma_k}-2m_N^2+2E_NE'_N}{2(E_N+m_N)(E'_N+m_N)}\right)\ln\left(\frac{2p_{cm}p'_{cm}-m^2_{\sigma_k}+2m_N^2-2E_NE'_N}{-2p_{cm}p'_{cm}-m^2_{\sigma_k}+2m_N^2-2E_NE'_N}\right)\Bigg\}$$
$$+\frac{g_{\eta_i N}g_{\eta_j N}}{W^2-m_N^2}\left(E_i+\frac{p^2_{cm}}{E_N+m_N}\right)+g_{\eta_i N}g_{\eta_j N}\left\{\frac{W+m_N}{2(E_N+m_N)(E'_N+m_N)}\right.$$
$$+\frac{1}{4p_{cm}p'_{cm}}\left(E_j+\frac{p'^2_{cm}}{E'_N+m_N}-\frac{(W+m_N)(2E_NE_j-m_j^2)}{2(E_N+m_N)(E'_N+m_N)}\right)$$
$$\left.\left.\cdot\ln\left(\frac{2p_{cm}p'_{cm}+2E_NE_j-m_j^2}{-2p_{cm}p'_{cm}+2E_NE_j-m_j^2}\right)\right\}\right]. \tag{B6}$$

Then, the explicit form of $V_{i\to j}$ ($i,j=\eta' N,\eta N$, or πN) is:

$$V_{\eta' N\to\eta' N} = -\sum_{\sigma_k}\frac{g_{\eta' N}g_{\eta'\eta'\sigma_k}}{m^2_{\sigma_k}}+\frac{4m_Ng^2_{\eta' N}}{4m_N^2-m^2_{\eta'}}, \tag{B7}$$

$$V_{\eta_i N\to\eta_i N} = \frac{E_N+m_N}{2m_N}\left[\sum_{\sigma_k}g_{\sigma_k\eta_i\eta_i}g_{\sigma_k N}\left\{-\frac{1}{2(E_N+m_N)^2}+\frac{1}{4p'^2_{cm}}\left(1-\frac{m^2_{\sigma_k}+2p^2_{cm}}{2(E_N+m_N)^2}\right)\right.\right.$$
$$\cdot\ln\left(\frac{m^2_{\sigma_k}}{m^2_{\sigma_k}+4p^2_{cm}}\right)+\frac{g^2_{\eta_i N}\left(E_i+\frac{p^2_{cm}}{E_N+m_N}\right)}{W^2-m_N^2}+g^2_{\eta_i N}\left\{\frac{W+m_N}{2(E_N+m_N)^2}+\frac{1}{4p^2_{cm}}\right.$$
$$\cdot\left(E_i+\frac{p^2_{cm}}{E_N+m_N}-\frac{(W+m_N)(2E_NE_i-m_i^2)}{2(E_N+m_N)^2}\right)$$
$$\left.\left.\left.\cdot\ln\left(\frac{2p^2_{cm}+2E_NE_i-m_i^2}{-2p^2_{cm}+2E_NE_i-m_i^2}\right)\right\}\right] \quad(\eta_i=\pi^0,\eta), \tag{B8}$$

$$V_{\pi^+n\to\pi^+n} = \frac{E_N+m_N}{2m_N}\left[\sum_{\sigma_k}g_{\sigma_k\pi^+\pi^-}g_{\sigma_k N}\left\{-\frac{1}{2(E_N+m_N)^2}\right.\right.$$
$$\left.\left.+\frac{1}{4p'^2_{cm}}\left(1-\frac{m^2_{\sigma_k}+2p^2_{cm}}{2(E_N+m_N)^2}\ln\left(\frac{m^2_{\sigma_k}}{m^2_{\sigma_k}+4p^2_{cm}}\right)\right)\right\}+\frac{g^2_{\pi^+n}\left(E_i+\frac{p^2_{cm}}{E_N+m_N}\right)}{W^2-m_N^2}\right], \tag{B9}$$

$$V_{\pi^+p\to\pi^+p} = \frac{E_N+m_N}{2m_N}\left[\sum_{\sigma_k}g_{\sigma_k\pi^+\pi^-}g_{\sigma_k N}\left\{-\frac{1}{2(E_N+m_N)^2}\right.\right.$$
$$\left.+\frac{1}{4p'^2_{cm}}\left(1-\frac{m^2_{\sigma_k}+2p^2_{cm}}{2(E_N+m_N)^2}\ln\left(\frac{m^2_{\sigma_k}}{m^2_{\sigma_k}+4p^2_{cm}}\right)\right)\right\}+g^2_{\pi^+p}\left\{\frac{W+m_N}{2(E_N+m_N)}\right.$$
$$\left.\left.+\frac{1}{4p^2_{cm}}\left(E_i+\frac{p^2_{cm}}{E_N+m_N}-\frac{(W+m_N)(2E_NE_i-m_i^2)}{2(E_N+m_N)^2}\right)\right.\right.$$

$$\cdot \ln\left(\frac{2p_{cm}^2+2E_NE_i-m_i^2}{-2p_{cm}^2+2E_NE_i-m_i^2}\right)\Bigg\}\Bigg], \tag{B10}$$

$$V_{\eta'N\to\eta_jN}=\sqrt{\frac{E'_N+m_N}{2m_N}}\left[\sum_{\sigma_k}g_{\eta'N}g_{\eta'\eta_j\sigma_k}\left\{-\frac{1}{4m_N(E'_N+m_N)}+\frac{1-\frac{m_{\sigma_k}^2-2m_N^2+2m_NE'_N}{4m_N(E'_N+m_N)}}{2m_N^2-m_{\sigma_k}^2-2m_NE'_N}\right\}\right.$$
$$\left.+\frac{g_{\eta'N}g_{\eta_jN}}{2m_N+m_{\eta'}}+g_{\eta'N}g_{\eta_jN}\frac{\left(E_j+\frac{p'^2_{cm}}{E'_N+m_N}\right)}{2m_NE_j-m_j^2}\right]\quad(\eta_j=\pi^0,\eta), \tag{B11}$$

$$V_{\pi^+n\to\pi^0p}=\frac{E_N+m_N}{2m_N}\left[\sum_{\sigma_k}g_{\sigma_k\pi^+\pi^0}g_{\sigma_kN}\left\{-\frac{1}{2(E_N+m_N)^2}\right.\right.$$
$$\left.+\frac{1}{4p'^2_{cm}}\left(1-\frac{m_{\sigma_k}^2+2p_{cm}^2}{2(E_N+m_N)^2}\right)\ln\left(\frac{m_{\sigma_k}^2}{m_{\sigma_k}^2+4p_{cm}^2}\right)\right\}+\frac{g_{\pi^+N}g_{\pi^0p}\left(E_i+\frac{p_{cm}^2}{E_N+m_N}\right)}{W^2-m_N^2}$$
$$+g_{\pi^+N}g_{\pi^0n}\left\{\frac{W+m_N}{2(E_N+m_N)^2}+\frac{1}{4p_{cm}^2}\left(E_i+\frac{p_{cm}^2}{E_N+m_N}-\frac{(W+m_N)(2E_NE_i-m_i^2)}{2(E_N+m_N)^2}\right)\right.$$
$$\left.\left.\cdot\ln\left(\frac{2p_{cm}^2+2E_NE_i-m_i^2}{-2p_{cm}^2+2E_NE_i-m_i^2}\right)\right\}\right], \tag{B12}$$

$$V_{\eta N\to\pi N}=\frac{\sqrt{(E_N+m_N)(E'_N+m_N)}}{2m_N}\left[\sum_{\sigma_k}\left\{-\frac{1}{2(E_N+m_N)(E'_N+m_N)}\right.\right.$$
$$\left.+\frac{1}{4p_{cm}p'_{cm}}\left(1-\frac{m_{\sigma_k}^2-2m_N^2+2E_NE'_N}{2(E_N+m_N)(E'_N+m_N)}\right)\cdot\ln\left(\frac{2p_{cm}p'_{cm}-m_{\sigma_k}^2+2m_N^2-2E_NE'_N}{-2p_{cm}p'_{cm}-m_{\sigma_k}^2+2m_N^2-2E_NE'_N}\right)\right\}$$
$$+\frac{g_{\eta N}g_{\pi N}}{W^2-m_N^2}\left(E_i+\frac{p_{cm}^2}{E_N+m_N}\right)+g_{\eta N}g_{\pi N}\left\{\frac{W+m_N}{2(E_N+m_N)(E'_N+m_N)}+\frac{1}{4p_{cm}p'_{cm}}\right.$$
$$\left.\left.\cdot\left(E_j+\frac{p'^2_{cm}}{E'_N+m_N}-\frac{(W+m_N)(2E_NE_j-m_j^2)}{2(E_N+m_N)(E'_N+m_N)}\right)\ln\left(\frac{2p_{cm}p'_{cm}+2E_NE'_N-m_j^2}{-2p_{cm}p'_{cm}+2E_NE_j-m_j^2}\right)\right\}\right]. \tag{B13}$$

The transition term $V_{\eta^{(\prime)}p\to\pi^+n}$ satisfies $V_{\eta^{(\prime)}p\to\pi^+n}=V_{\eta^{(\prime)}n\to\pi^-p}=\sqrt{2}V_{\eta^{(\prime)}p\to\pi^0p}=-\sqrt{2}V_{\eta^{(\prime)}n\to\pi^0n}$. The transition term from $\eta^{(\prime)}N$ to πN $(I=1/2)$ is given as

$$V_{\eta^{(\prime)}N\to\pi N(I=1/2,I_z=1/2)}=\frac{1}{\sqrt{3}}\left(V_{\eta^{(\prime)}p\to\pi^0p}+\sqrt{2}V_{\eta^{(\prime)}p\to\pi^+n}\right), \tag{B14}$$

$$V_{\eta^{(\prime)}N\to\pi N(I=1/2,I_z=-1/2)}=-\frac{1}{\sqrt{3}}\left(V_{\eta^{(\prime)}n\to\pi^0n}-\sqrt{2}V_{\eta^{(\prime)}n\to\pi^-p}\right). \tag{B15}$$

Then, $V_{\eta^{(\prime)}N\to\pi N(I=1/2)}$ is given as $V_{\eta^{(\prime)}N\to\pi N(I=1/2,I_z=\pm1/2)}=\sqrt{3}V_{\eta'N\to\pi^0N}$. For the πN $(I=1/2)$ elastic channel, the matrix element is written as

$$V_{\pi N\to\pi N(I=1/2,I_z=1/2)}=\frac{1}{3}\left(V_{\pi^0p\to\pi^0p}+\sqrt{2}V_{\pi^0p\to\pi^+n}+\sqrt{2}V_{\pi^+n\to\pi^0p}+2V_{\pi^+n\to\pi^+n}\right), \tag{B16}$$

$$V_{\pi N\to\pi N(I=1/2,I_z=-1/2)} = \frac{1}{3}\left(V_{\pi^0 n\to\pi^0 n} - \sqrt{2}V_{\pi^0 n\to\pi^- p} - \sqrt{2}V_{\pi^- p\to\pi^0 n} + 2V_{\pi^- p\to\pi^- p}\right). \tag{B17}$$

Here, $V_{\pi^0 p\to\pi^+ n} = -V_{\pi^0 n\to\pi^- p}$, $V_{\pi^0 n\to\pi^0 n} = V_{\pi^0 p\to\pi^0 p}$, and $V_{\pi^+ n\to\pi^+ n} = V_{\pi^- p\to\pi^- p}$. Then, $V_{\pi N\to\pi N(I=1/2,I_z=1/2)} = V_{\pi N\to\pi N(I=1/2,I_z=-1/2)}$ is satisfied.

Appendix C. Couplings of hadrons

In this appendix, we present the couplings of the hadrons appearing in the text. The couplings of the meson (σ_i or η_i) and nucleon are summarized in Table C.1. $g_{\sigma_i N}$ and $g_{\eta_i N}$ denote the coefficients of the terms $\bar{N}\sigma_i N$ and $\bar{N}\eta_i\gamma_5 N$ in the Lagrangian Eq. (1), respectively.

The couplings of the mesons $g_{\sigma_i\eta_j\eta_k}$, which are defined as the coefficients of the term $\sigma_i\eta_j\eta_k$ in the Lagrangian, are given in Table C.2. The parameters a, b, and c in the table characterize the coupling of the meson as

$$g_{\sigma_i\eta_j\eta_k} = -(a\lambda + b\lambda' + cB). \tag{C1}$$

Due to the isospin symmetry, $g_{\sigma_{0,3,8}\pi^\pm\pi^\mp} = g_{\sigma_{0,3,8}\pi_3\pi_3}$, $g_{a_0^\pm\eta_0\pi^\mp} = g_{\sigma_3\eta_0\pi_3}$, and $g_{a_0^\pm\pi^\mp\eta_8} = g_{\sigma_3\pi_3\eta_8}$, and the couplings $g_{\sigma_3\eta_{0,8}\eta_{0,8}}$ and $g_{\sigma_{0,8}\pi_3\eta_{0,8}}$ vanish. Here, η_i and σ_i are the eigenstates of the Gell-Mann matrix appearing in the Lagrangian, and these states are mixed by the flavor SU(3) symmetry breaking. The eigenstates of the mass σ, f_0, η', and η and the Gell-Mann matrix σ_i and η_i ($i = 0, 8$) are related by the matrices in Eqs. (8) and (9), respectively. The coupling of σ (η') and f_0 (η) to the hadronic state h in the mass eigenstate is obtained using the mixing angles θ_s and θ_{ps} for the scalar

Table C.1. Meson–baryon couplings. τ_3 is the third component of the Pauli matrix.

$g_{\sigma_0 N}$	$g_{\sigma_3 N}$	$g_{\sigma_8 N}$	$g_{a_0^\pm N}$	$g_{\eta_0 N}$	$g_{\pi_3 N}$	$g_{\eta_8 N}$	$g_{\pi^\pm N}$
$-g/\sqrt{3}$	$-g\tau_3/\sqrt{2}$	$-g/\sqrt{6}$	$-g$	$g/\sqrt{3}$	$g\tau_3/\sqrt{2}$	$g/\sqrt{6}$	g

Table C.2. Meson couplings. a, b, and c are defined by $g_{\sigma_i\eta_j\eta_k} = -(a\lambda + b\lambda' + cB)$, where λ, λ', and B are the parameters appearing in the Lagrangian.

	a	b	c
$g_{\sigma_0\eta_0\eta_0}$	$\frac{2}{3}\langle\sigma_0\rangle$	$2\langle\sigma_0\rangle$	4
$g_{\sigma_8\eta_0\eta_0}$	$\frac{2}{3}\langle\sigma_8\rangle$	$2\langle\sigma_8\rangle$	0
$g_{\sigma_0\pi_3\pi_3}$	$\frac{2}{3}(\langle\sigma_0\rangle + \frac{\langle\sigma_8\rangle}{\sqrt{2}})$	$2\langle\sigma_0\rangle$	-2
$g_{\sigma_3\pi_3\pi_3}$	0	0	0
$g_{\sigma_8\pi_3\pi_3}$	$\frac{\sqrt{2}}{3}(\langle\sigma_0\rangle + \frac{\langle\sigma_8\rangle}{\sqrt{2}})$	$2\langle\sigma_8\rangle$	$2\sqrt{2}$
$g_{a_0^\pm\pi_3\pi^\mp}$	0	0	0
$g_{\sigma_0\eta_8\eta_8}$	$\frac{2}{3}(\langle\sigma_0\rangle - \frac{\langle\sigma_8\rangle}{\sqrt{2}})$	$2\langle\sigma_0\rangle$	-2
$g_{\sigma_8\eta_8\eta_8}$	$-\frac{\sqrt{2}}{3}(\langle\sigma_0\rangle - \frac{3}{\sqrt{2}}\langle\sigma_8\rangle)$	$2\langle\sigma_8\rangle$	$-2\sqrt{2}$
$g_{\sigma_0\eta_0\eta_8}$	$\frac{2}{3}\langle\sigma_8\rangle$	0	0
$g_{\sigma_8\eta_0\eta_8}$	$\frac{2}{3}(\langle\sigma_0\rangle - \frac{\langle\sigma_8\rangle}{\sqrt{2}})$	0	-2
$g_{\sigma_3\eta_0\pi_3}$	$\frac{2}{3}(\langle\sigma_0\rangle + \frac{\langle\sigma_8\rangle}{\sqrt{2}})$	0	-2
$g_{\sigma_3\pi_3\eta_8}$	$\frac{\sqrt{2}}{3}(\langle\sigma_0\rangle + \frac{\langle\sigma_8\rangle}{\sqrt{2}})$	0	$2\sqrt{2}$

and pseudoscalar mesons:

$$g_{\sigma(\eta')h} = \cos\theta_{s(ps)} g_{\sigma_0(\eta_0)h} + \sin\theta_{s(ps)} g_{\sigma_8(\eta_8)h}, \tag{C2}$$

$$g_{f_0(\eta)h} = -\sin\theta_{s(ps)} g_{\sigma_0(\eta_0)h} + \cos\theta_{s(ps)} g_{\sigma_8(\eta_8)h}. \tag{C3}$$

References

[1] S. Weinberg, Phys. Rev. D **11**, 3583 (1975).
[2] G. 't Hooft, Phys. Rept. **142**, 357 (1986).
[3] G. A. Christos, Phys. Rept. **116**, 251 (1984).
[4] E. Witten, Nucl. Phys. B **156**, 269 (1979).
[5] G. Veneziano, Nucl. Phys. B **159**, 213 (1979).
[6] S. L. Adler, Phys. Rev. **177**, 2426 (1969).
[7] J. S. Bell and R. Jackiw, Nuovo Cim. A **60**, 47 (1969).
[8] W. A. Bardeen, Phys. Rev. **184**, 1848 (1969).
[9] R. D. Pisarski and F. Wilczek, Phys. Rev. D **29**, 338 (1984).
[10] H. Kikuchi and T. Akiba, Phys. Lett. B **200**, 543 (1988).
[11] T. Kunihiro and T. Hatsuda, Phys. Lett. B **206**, 385 (1988); **210**, 278 (1988) [erratum].
[12] T. D. Cohen, Phys. Rev. D **54**, 1867 (1996).
[13] S. H. Lee and T. Hatsuda, Phys. Rev. D **54**, 1871 (1996).
[14] D. Jido, H. Nagahiro, and S. Hirenzaki, Phys. Rev. C **85**, 032201(R) (2012).
[15] E. G. Drukarev and E. M. Levin, Prog. Part. Nucl. Phys. **27**, 77 (1991).
[16] T. D. Cohen, R. J. Furnstahl, and D. K. Griegel, Phys. Rev. C **45**, 1881 (1992).
[17] R. Brockmann and W. Weise, Phys. Lett. B **367**, 40 (1996).
[18] R. S. Hayano and T. Hatsuda, Rev. Mod. Phys. **82**, 2949 (2010).
[19] K. Suzuki et al., Phys. Rev. Lett. **92**, 072302 (2004).
[20] E. Friedman et al., Phys. Rev. Lett. **93**, 122302 (2004).
[21] E. E. Kolomeitsev, N. Kaiser, and W. Weise, Phys. Rev. Lett. **90**, 092501 (2003).
[22] D. Jido, T. Hatsuda, and T. Kunihiro, Phys. Lett. B **670**, 109 (2008).
[23] T. Kunihiro, Phys. Lett. B **219**, 363 (1989).
[24] J. I. Kapusta, D. Kharzeev, and L. D. McLerran, Phys. Rev. D **53**, 5028 (1996).
[25] P. Costa, M. C. Ruivo, and Yu. L. Kalinovsky, Phys. Lett. B **560**, 171 (2003).
[26] H. Nagahiro, M. Takizawa, and S. Hirenzaki, Phys. Rev. C **74**, 045203 (2006).
[27] S. Sakai and D. Jido, Phys. Rev. C **88**, 064906 (2013).
[28] K. Tsushima, D.-H. Lu, A. W. Thomas, and K. Saito, Phys. Lett. B **443**, 26 (1998).
[29] K. Tsushima, D.-H. Lu, A. W. Thomas, K. Saito, and R. H. Landau, Phys. Rev. C **59**, 2824 (1999).
[30] K. Tsushima, Nucl. Phys. A **670**, 198 (2000).
[31] H. Nagahiro and S. Hirenzaki, Phys. Rev. Lett. **94**, 232503 (2005).
[32] H. Nagahiro, S. Hirenzaki, E. Oset, and A. Ramos, Phys. Lett. B **709**, 87 (2012).
[33] M. Nanova et al., Phys. Lett. B **710**, 600 (2012).
[34] K. Itahashi et al., Prog. Theor. Phys. **128**, 601 (2012).
[35] H. Nagahiro, D. Jido, H. Fujioka, K. Itahashi, and S. Hirenzaki, Phys. Rev. C **87**, 045201 (2013).
[36] M. Nanova et al. [CBELSA/TAPS Collaboration], Phys. Lett. B **727**, 417 (2013).
[37] S. D. Bass and A. W. Thomas, Phys. Lett. B **634**, 368 (2006).
[38] K. Kawarabayashi and N. Ohta, Prog. Theor. Phys. **66**, 1789 (1981).
[39] B. Borasoy, Phys. Rev. D **61**, 014011 (2000).
[40] E. Oset and A. Ramos, Phys. Lett. B **704**, 334 (2011).
[41] P. G. Moyssides et al., Nuovo Cim. A **75**, 163 (1983).
[42] V. L. Kashevarov, L. Tiator, and M. Ostrick, Bled Workshops Phys. **16**, 9 (2015).
[43] P. Moskal et al., Phys. Lett. B **474**, 416 (2000).
[44] P. Moskal et al., Phys. Lett. B **482**, 356 (2000).
[45] E. Czerwinski et al., Phys. Rev. Lett. **113**, 062004 (2014).
[46] S. Sakai and D. Jido, Hyperfine Interact. **234**, 71 (2015).
[47] T. Sekihara, S. Sakai and D. Jido, Phys. Rev. C **94**, 025203 (2016).

[48] K. A. Olive et al. [Particle Data Group Collaboration], Chin. Phys. C **38**, 090001 (2014).
[49] T. Inoue, E. Oset, and M. J. Vicente Vacas, Phys. Rev. C **65**, 035204 (2002).
[50] T. Hyodo, D. Jido, and A. Hosaka, Phys. Rev. C **78**, 025203 (2008).
[51] R. K. Rader et al., Phys. Rev. D **6**, 3059 (1972).
[52] Y. Ikeda, T. Hyodo, D. Jido, H. Kamano, T. Sato, and K. Yazaki, Prog. Theor. Phys. **125**, 1205 (2011).